WASP-28b: a hot Jupiter transiting a low-metallicity star

R. G. West[1]

D. R. Anderson[2]

D. J. A. Brown[3]

A. Collier Cameron[3]

M. Gillon[4]

C. Hellier[2]

T. A. Lister[5]

P. F. L. Maxted[2]

D. Queloz[6]

B. Enoch[3]

N. Parley[3]

F. Pepe[6]

D. Pollacco[7]

D. Segransan[6]

B. Smalley[2]

A. H. M. J. Triaud[6]

S. Udry[6]

P. J. Wheatley[8]

Received _____; accepted _____

[1]Department of Physics and Astronomy, University of Leicester, Leicester, LE1 7RH, UK

[2]Astrophysics Group, Keele University, Staffordshire, ST5 5BG, UK

[3]School of Physics and Astronomy, University of St. Andrews, North Haugh, Fife, KY16 9SS, UK

[4]Institut d'Astrophysique et de Géophysique, Université de Liège, Allée du 6 Août, 17, Bat. B5C, Liège 1, Belgium

[5]Las Cumbres Observatory, 6740 Cortona Dr. Suite 102, Santa Barbara, CA 93117, USA

[6]Observatoire de Genève, Université de Genève, 51 Chemin des Maillettes, 1290 Sauverny, Switzerland

[7]Astrophysics Research Centre, School of Mathematics & Physics, Queen's University, University Road, Belfast, BT7 1NN, UK

[8]Department of Physics, University of Warwick, Coventry, CV4 7AL, UK

ABSTRACT

We report the discovery of a transiting exoplanet in a 3.408 day orbit about an early G-type star. The host star has a mass of $1.08 \pm 0.04 M_{\odot}$, a radius of $1.05 \pm 0.06 R_{\odot}$, an effective temperature of 6100 ± 150K, and a metallicity $[Fe/H] = -0.29 \pm 0.10$ which is amongst the lowest measured for the host star of a transiting exoplanet. We combine the available spectral and photometric data to measure the planet's mass of $0.91 \pm 0.06 M_{J}$ and radius of $1.12 \pm 0.06 R_{J}$. We find the measured radius to be consistent with theoretical evolutionary models of an irradiated planet with a low heavy element content.

Subject headings: binaries: eclipsing — stars: individual (WASP-28) — planetary systems — techniques: photometric — techniques: radial velocities — techniques: spectroscopic

1. Introduction

Transiting exoplanets provide a unique opportunity to study the internal structure and composition of planetary-mass objects, allowing as they do the determination of the mass and radius of the planet to an accuracy often limited only by the knowledge of the properties of the host star. The measured mass and radius can then be compared with theoretical models of planetary evolution to gain an insight into the internal structure of the planet. To date, the discoveries have been announced of more than 70 transiting exoplanets by the various survey projects[1].

The WASP project operates two observatories, one at La Palma in the Canary Islands, and the other at Sutherland in South Africa. Each telescope has a field of view of approximately 500 square degrees. The WASP survey is capable of detecting planetary transit signatures in the light-curves of hosts in the magnitude range V ∼9–13. A full description of the telescope hardware, observing strategy and pipeline data analysis is given in Pollacco et al. (2006).

2. Observations

The host star WASP-28 (1SWASP J233427.87-013448.1 = 2MASS 23342787-0134482) has a catalogued magnitude V = 12.0. It was observed by WASP-South from 2008 June 06 through 2008 Nov 17, and by WASP-North from 2008 July 19 through 2008 Nov 30, with a total of 7837 photometric points acquired during these intervals. These data were pipeline processed, de-trended and searched for transit signatures as described in Collier Cameron et al. (2006), yielding the detection of a transit-like signal with a period of 3.408 days. The WASP discovery photometry is shown in Figure 1 (top panel).

[1]http://www.exoplanet.eu

Photometric follow-up observations were made on 2009 Oct 22 using the LCOGT 2.0m Faulkes Telescope North (FTN, Maui, Hawai'i) using the Merope instrument and the Pan-STARRS-z filter. The Merope instrument contains a deep-depletion e2v 2048 × 2048 pixel CCD which was binned 2 × 2 giving 0.278″ pixels and a field of view of 4.7′ × 4.7′. The telescope was defocussed during the observations to prevent saturation and to increase the exposure and reduce the effect of scintillation. The DAOPHOT photometry package within IRAF[2] was used to perform object detection and aperture photometry using a 15 pixel aperture radius. Differential photometry was performed relative to 7 comparison stars within the field of view. The light-curve (Figure 1, lower panel) confirms the presence of a transit. The in-transit photometry shows some structure which proved resistant to repeated attempts to remove it through re-analysis the data; the source of this excess variation is unknown, it may be due to atmospheric or instrumental effects, or rather less likely due to stellar activity.

Radial velocity follow-up was performed using the CORALIE spectrograph on the 1.2m Euler telescope between 2009 Jun 23 and 2009 Oct 24, with total of 18 radial velocity measurements were obtained. These measurements show a radial velocity semi-amplitude of $116\,\mathrm{m\,s^{-1}}$ on the same period as the transit, which is consistent with the presence of a planet-mass companion (Figure 2, top panel). There is no evidence of a correlation between radial velocity and the bisector spans (Figure 2, lower panel) that might be expected if the radial velocity changes were due to a line-of-sight blend with an eclipsing binary (Queloz et al. 2001).

[2]`IRAF` is distributed by the National Optical Astronomy Observatory, which is operated by the Association of Universities for Research in Astronomy, Inc., under cooperative agreement with the National Science Foundation.

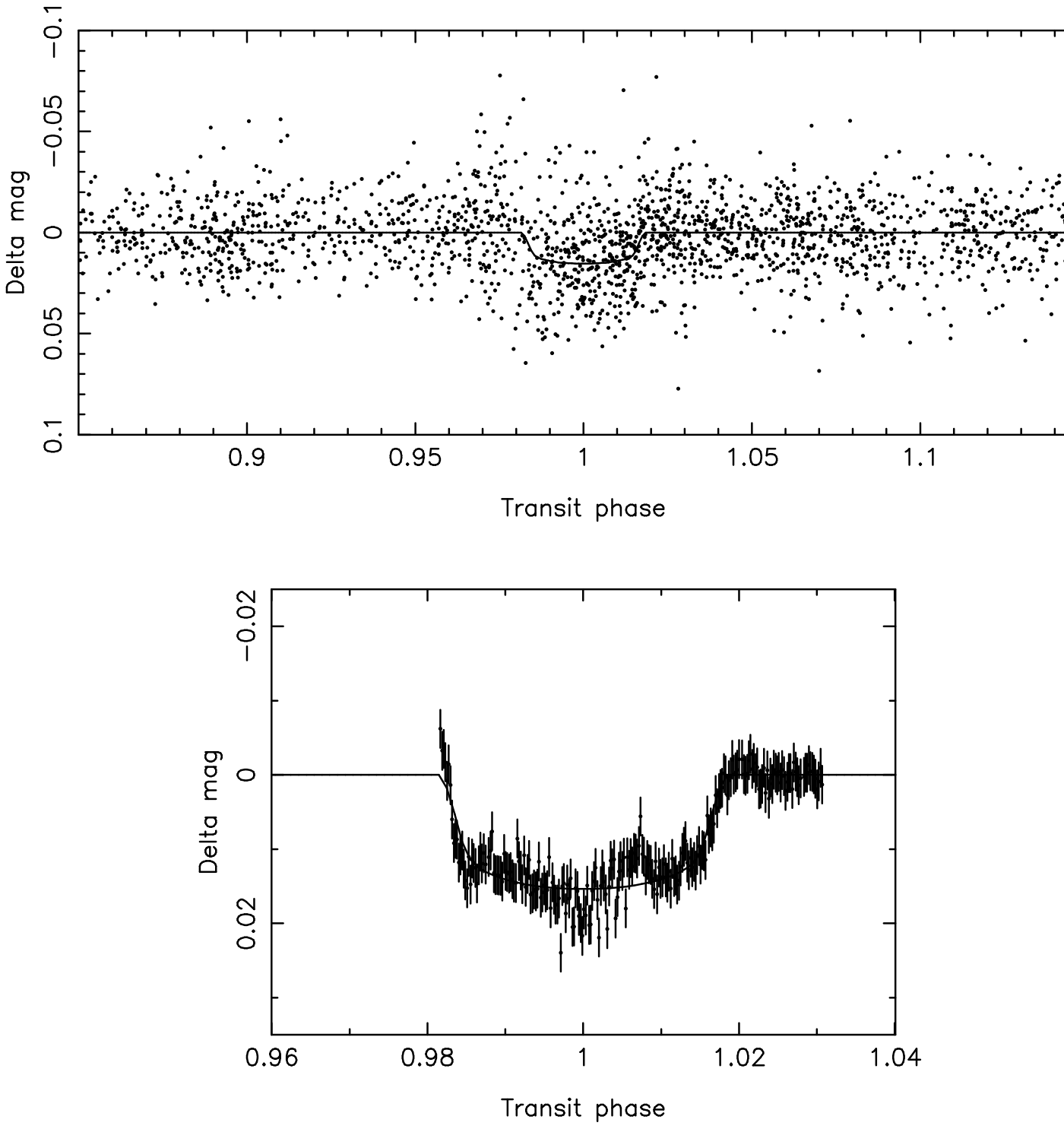

Fig. 1.— WASP photometry folded on the best-fit period (top panel). FTS PannSTARRS z-band follow-up photometry is shown in the lower panel. Curve shows the best-fit transit model from the MCMC fitting.

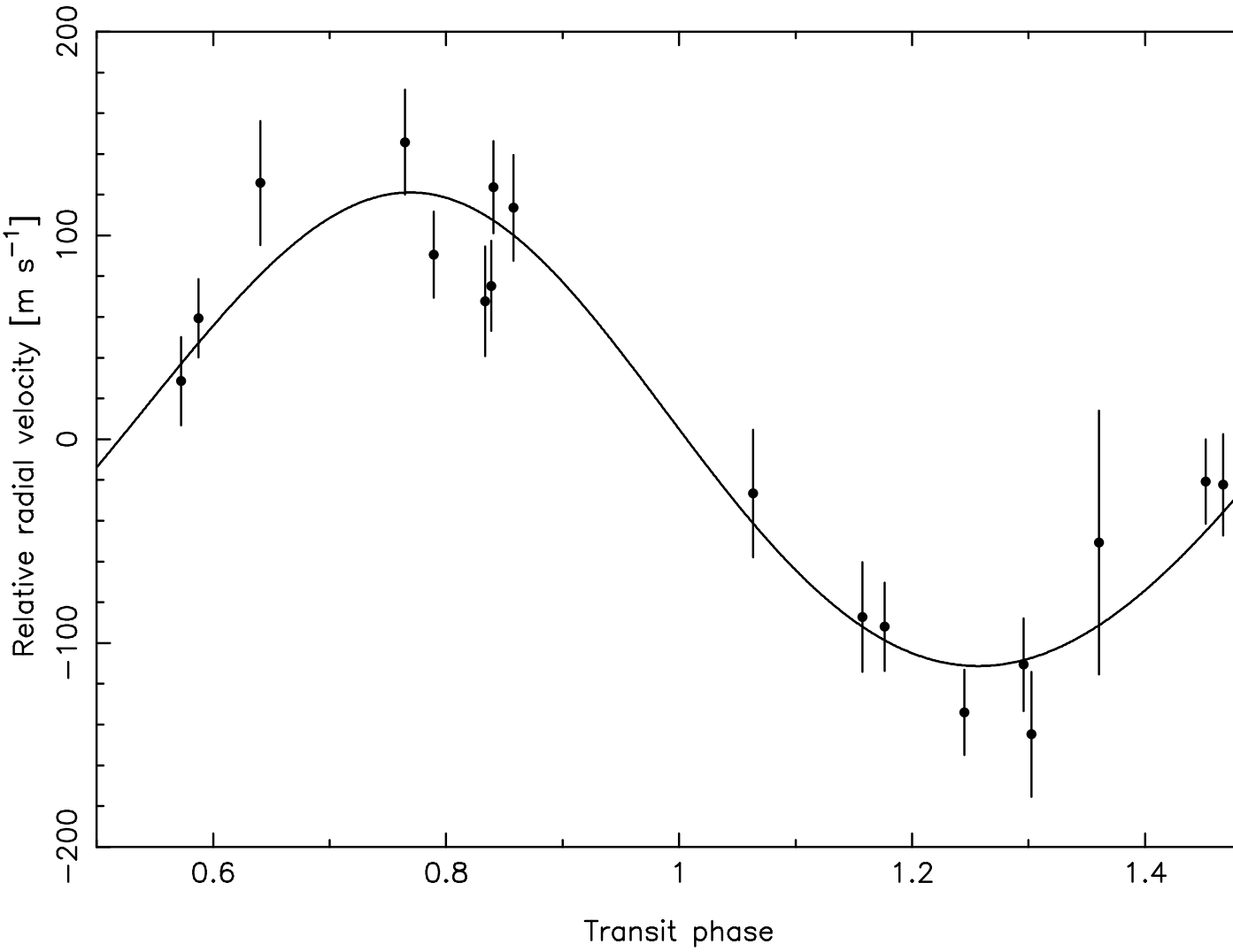

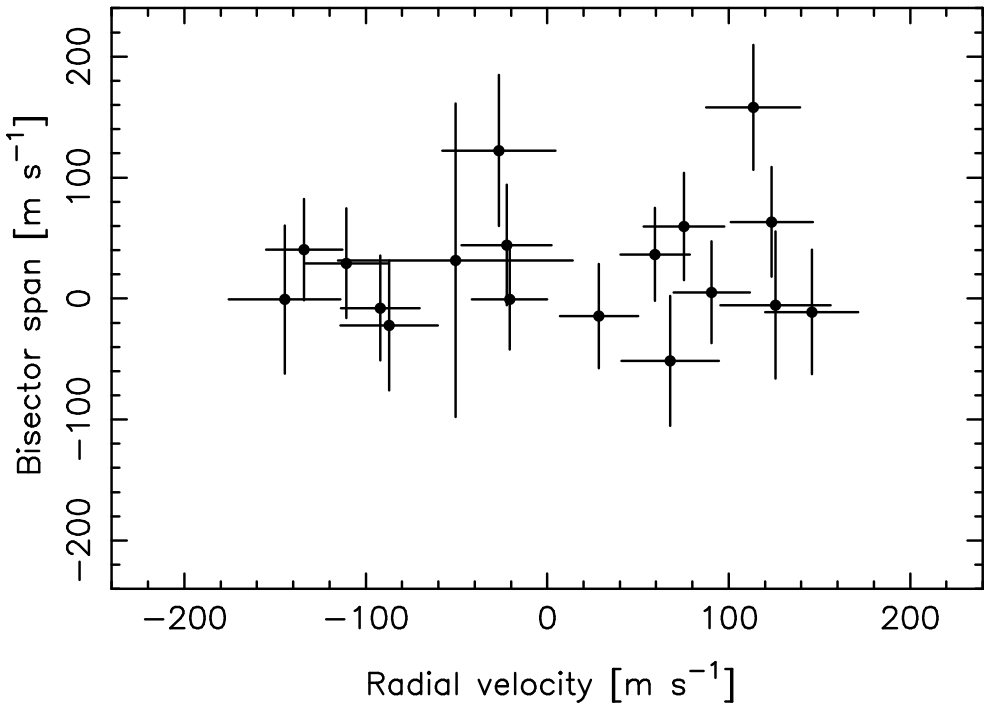

Fig. 2.— Radial velocity measurements of WASP-28 from CORALIE. The centre-of-mass

Table 1. Radial velocity measurements of WASP-28

BJD −2 400 000	RV (km s^{-1})	$\sigma_{\rm RV}$ (km s^{-1})	BS (km s^{-1})
55006.9078	24.285	0.027	−0.052
55011.9151	24.072	0.031	0.001
55064.7064	24.307	0.021	0.005
55069.6685	24.083	0.021	0.041
55070.7848	24.245	0.022	−0.014
55071.6932	24.292	0.022	0.060
55072.7796	24.130	0.027	−0.022
55073.8349	24.195	0.025	0.044
55074.8492	24.363	0.026	−0.011
55075.8674	24.190	0.031	0.122
55076.8806	24.166	0.065	0.031
55093.7037	24.106	0.023	0.029
55094.6979	24.276	0.019	0.036
55095.6190	24.330	0.026	0.158
55096.7056	24.125	0.022	−0.008
55097.6457	24.196	0.021	0.001
55118.7411	24.343	0.030	−0.005
55129.6486	24.341	0.023	0.063

Table 2. Stellar and system parameters of WASP-28

Parameter	Value
Stellar mass, M_* ($M_\odot$)	1.08 ± 0.04
Stellar radius, R_* ($R_\odot$)	1.05 ± 0.06
Stellar surface gravity, $\log g^{\rm a}$ (cgs)	4.43 ± 0.04
Mean stellar density, ρ_* ($\rho_\odot$)	0.93 ± 0.13
$T_{\rm eff}$ (K)	6100 ± 150
$\log g^{\rm b}$	4.5 ± 0.2
$\xi_{\rm t}$ ($\mathrm{km\,s^{-1}}$)	1.2 ± 0.1
$v \sin i$ ($\mathrm{km\,s^{-1}}$)	2.2 ± 1.6
[Fe/H]	-0.29 ± 0.10
[Si/H]	-0.22 ± 0.10
[Ca/H]	-0.20 ± 0.12
[Ti/H]	-0.21 ± 0.07
[Ni/H]	-0.28 ± 0.08
log A(Li)	2.52 ± 0.12
Transit epoch (BJD), $T_{\rm c}$	2455116.5573 ± 0.0005
Orbital period, P (d)	3.408821 ± 0.000015
Transit duration, T_{14} (d)	0.1267 ± 0.0013
Planet/star area ratio, $R_{\rm p}^2/{\rm R}_*^2$	0.0120 ± 0.0005
Stellar reflex vel., K_1 ($\mathrm{m\ s^{-1}}$)	116.2 ± 7.5
Centre-of-mass vel., γ ($\mathrm{km\ s^{-1}}$)	24.2169 ± 0.0008
Orbital separation, a (AU)	0.0455 ± 0.0005

3. Stellar parameters of the host star

A total of 18 individual CORALIE spectra of WASP-28 were co-added to produce a single spectrum with a typical S/N of around 70:1. The standard pipeline reduction products were used in the analysis. The analysis was performed using the methods given in Gillon et al. (2009). The H_α line was used to determine the effective temperature ($T_{\rm eff}$), while the Na I D and Mg I b lines were used as surface gravity ($\log g$) diagnostics. The parameters obtained from the analysis are listed in Table 2. The $T_{\rm eff}$ and $\log g$ are consistent with a spectral type around G0-F8. The elemental abundances were determined from equivalent width measurements of several clean and unblended lines. A value for microturbulence ($\xi_{\rm t}$) was determined from Fe I using the method of Magain (1984). The quoted error estimates include that given by the uncertainties in $T_{\rm eff}$, $\log g$ and $\xi_{\rm t}$, as well as the scatter due to measurement and atomic data uncertainties. The metallicity $[{\rm Fe/H}] = -0.29 \pm 0.10$ is amongst the lowest measured in stars known to host a transiting exoplanet, similar to the host stars of GJ436b (-0.32 ± 0.12, Bean et al. 2006), CoRoT-1b (-0.3 ± 0.25, Barge et al. 2008) and HAT-P-12 (-0.29 ± 0.05, Hartman et al. 2009).

The projected stellar rotation velocity ($v \sin i$) was determined by fitting the profiles of several unblended Fe I lines. A value for macroturbulence ($v_{\rm mac}$) of $4.7 \pm 0.3\,{\rm km\,s^{-1}}$ was assumed, based on the tabulation by Gray (2008), and an instrumental FWHM of 0.11 ± 0.01 Å, determined from the telluric lines around 6300 Å. A best fitting value of $v \sin i = 2.2 \pm 1.6\,{\rm km\,s^{-1}}$ was obtained.

In Figure 3 we compare the measured temperature and stellar density of WASP-28 with the theoretical evolutionary models of Girardi et al. (2000) interpolated to a metallicity of $[{\rm M/H}] = -0.29$. This shows that the probable age of the host star is in the range 5^{+3}_{-2} Gyr.

Table 2—Continued

Parameter	Value
Impact parameter, b	0.15 ± 0.11
Orbital inclination, i (°)	89.1 ± 0.6
Orbital eccentricity, e	0.046 ± 0.03
Planet mass, $M_{\rm p}$ ($M_{\rm J}$)	0.91 ± 0.06
Planet radius, $R_{\rm p}$ ($R_{\rm J}$)	1.12 ± 0.06
Planet surface gravity, $\log g_{\rm p}$ (cgs)	3.22 ± 0.05
Mean planetary density, $\rho_{\rm p}$ ($\rho_{\rm J}$)	0.65 ± 0.11
Planet equil. temp., $T_{\rm p,A=0}$ (K)	1410 ± 60
Safronov number, Θ	0.067 ± 0.006

[a]Derived from MCMC analysis

[b]Derived from spectral analysis

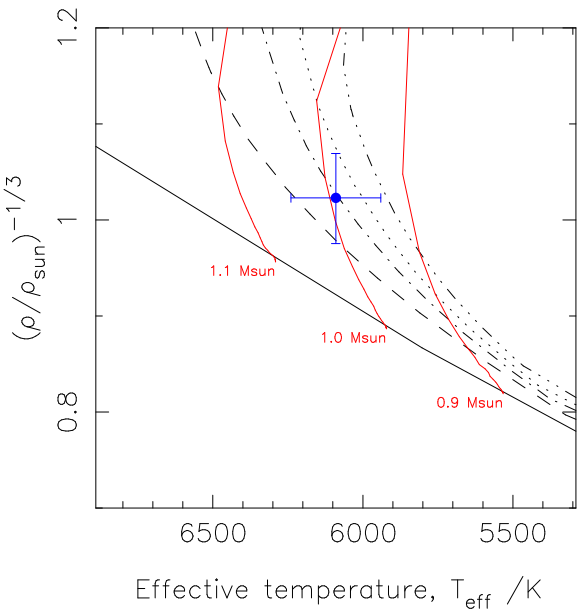

Fig. 3.— The location of the host star in the $(\rho_*/\rho_\odot)^{-1/3} - T_{\rm eff}$ plane, with theoretical evolutionary tracks from the model of Girardi et al. (2000) interpolated to [M/H] = −0.29. The isochrones shown are for 0.1 (solid), 3.16 (dashed), 5.01 (dot-dash), 6.30 (dotted) and 7.94 Gyr (triple dot-dash).

4. System parameters and discussion

The WASP and FTS photometry were fitted simultaneously with the CORALIE radial velocity measurements using the MCMC method (Collier Cameron et al. 2007). The best fitting stellar and system parameters are shown in Table 2, and reveal WASP-28b be a member of the "hot Jupiter" class. The best-fit orbital eccentricity is $e = 0.046 \pm 0.03$, is consistent with a circular orbit.

Figure 4 shows the measured mass and radius of WASP-28b compared to the models of Fortney et al. (2007) and Baraffe et al. (2008). For the Fortney models we account for the slightly higher than solar luminosity of the host star by interpolating to an effective orbital separation $a_{\odot} = 0.0398\,\mathrm{AU}$. For the Baraffe models no such adjustment can be made, and we note that the irradiation experienced by WASP-28b will be around 35% higher than assumed in those models, and that the modelled radii are therefore something of an under-estimate for this system. In both cases we find that at the best-fit age of the system ($\sim 5\,\mathrm{Gyr}$) the measured planetary parameters favour models with a low core mass ($M_{\mathrm{core}} \lesssim 10\mathrm{M}_{\oplus}$; $Z \lesssim 0.02$). A low heavy element content is in line with the observation that planetary core mass tends to correlate with the metallicity of the host star (Guillot et al. 2006; Burrows et al. 2007).

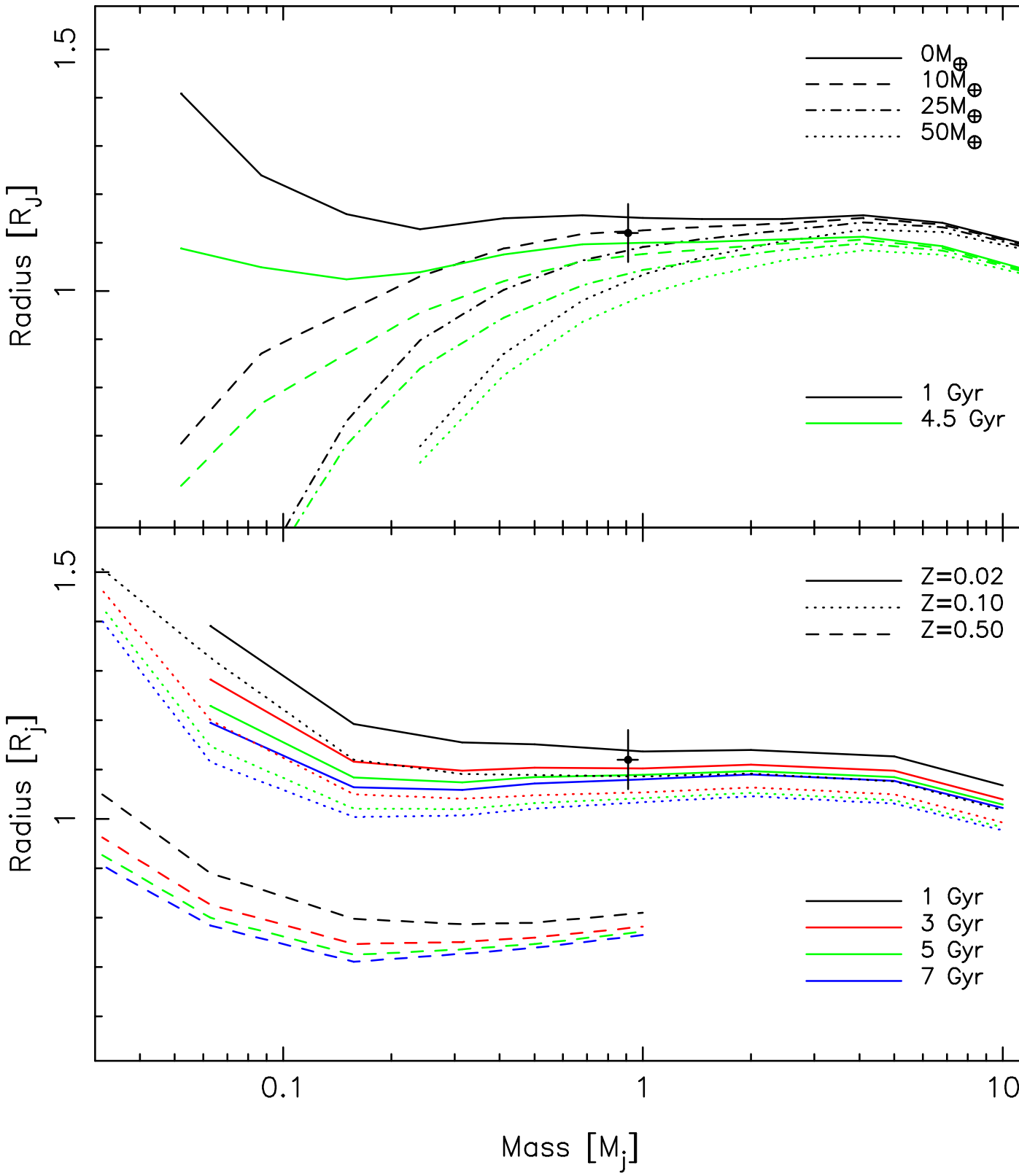

Fig. 4.— Top panel: mass-radius isochrones for an irradiated exoplanet from the models of Fortney et al. (2007) at ages of 1.0 (black) and 4.5 Gyr (green) with core masses of 0, 10, 25 and $50 M_{\oplus}$. Lower panel: models from Baraffe et al. (2008) at ages 1.0 (black), 3.0 (red), 5.0 (green) and 7.0 Gyr (blue) with metal fractions are $Z = 0.02$ (solid), $Z = 0.10$ (dotted) and $Z = 0.50$ (dashed).

REFERENCES

Baraffe, I., Chabrier, G., & Barman, T. 2008, A&A, 482, 513

Barge, P. et al, 2008, A&A, 482, L17

Bean, J.L., Benedict, G.F. & Endl, M., 2006, ApJ, 653, L65

Burrows, A., Hubeny, I., Budaj, J., & Hubbard, W.B. 2007, ApJ, 661, 502

Collier Cameron, A., et al. 2006, MNRAS, 373, 799

Collier Cameron, A., et al. 2007, MNRAS, 380, 1230

Fortney, J.J., Marley, M.S., & Barnes, J.W. 2007, ApJ, 659, 1661

Gillon, M. et al., 2009, A&A, 496, 259

Girardi, L., Bressan, A., Bertelli, G., & Chiosi, C. 2000, A&AS, 141, 371

Gray D.F., 2008, The observation and analysis of stellar photospheres, 3rd Edition, CUP, p. 507.

Guillot, T., Santos, N.C., Pont, F., Iro, N., Melo, C., & Ribas, I. 2006, A&A, 453, L21

Hartman, J. et al., 2009, ApJ, 706, 785

Magain P., 1984, A&A 134, 189

Pollacco, D. L., et al. 2006, PASP, 118, 1407

Queloz D., Henry G. W., Sivan J. P., et al., 2001, A&A, 379, 279

This manuscript was prepared with the AAS LaTeX macros v5.2.